Phospholipase D2 regulates endothelial permeability through cytoskeleton reorganization and occludin downregulation

Caroline Zeiller[a,b,c,d], Saïda Mebarek[a,b,c,d], Rami Jaafar[a,b,c,d], Luciano Pirola[a,b,c,d], Michel Lagarde[a,b,c,d], Annie-France Prigent[a,b,c,d] and Georges Némoz[a,b,c,d,*]

[a]Université de Lyon (Univ Lyon), F-69622, Lyon, France,
[b]INSERM U870, (IMBL) F-69621, Villeurbanne, France
[c]INSA-Lyon, RMND, F-69621, Villeurbanne,
[d]INRA, UMR1235, (Faculté Lyon-Sud) F-69921 Oullins,

Running head**:** PLD2 and endothelial permeability

Key words: stress fibres; lipid rafts; Raf-1 kinase; MAP kinases; phosphatidic acid

*Corresponding author: Georges Némoz, INSERM U870 INSA DE LYON, 11 avenue Jean Capelle, Bât. Louis Pasteur, IMBL, 69621 Villeurbanne Cedex, France.
Tel : (33)4 72 43 85 71, Fax : (33)4 72 43 85 24;
E-mail: georges.nemoz@insa-lyon.fr

Abstract

Endothelial permeability is controlled by adhesive strengths which connect cells to each other through interendothelial junctions and by contractile forces associated with cytoskeleton reorganization. Phospholipase D (PLD) activation resulting in the generation of phosphatidic acid (PA) is increasingly recognized as a key event in the initiation of various cell responses. In human umbilical vein endothelial cells (HUV-EC), enhancement of intracellular PA by a variety of approaches increased the permeability of endothelial cell monolayers and induced stress fibre formation. Using adenovirus-mediated overexpression and siRNA silencing, we showed that PLD2 but not PLD1 was involved in the enhancement of basal permeability through cytoskeleton reorganization. Furthermore, PLD2 overexpression induced ERK1/2 activation and downregulated the expression of occludin, a major component of tight junctions. A substantial part of PLD2 protein was associated with the low-density caveolin-rich fractions isolated on sucrose gradients. The Raf-1 specific inhibitor GW-5074 drastically reduced hyperpermeability induced by PLD2 overexpression, and inhibited PA-mediated increase of endothelial permeability and ERK1/2 activation. On the whole, the present results demonstrate the selective role of PLD2 isoform in the control of endothelial permeability through a mechanism involving both stress fibre formation and contraction, and occludin downregulation, possibly resulting from PA-mediated activation of Raf-1.

1. Introduction

Endothelial cells (ECs) form a semipermeable dynamic barrier that regulates the exchange of fluids and solutes between the vascular space and underlying tissues, and controls protein flux between the blood and subendothelial compartments [1,2]. Disruption of this semi-selective barrier is a hallmark of several pathological conditions including inflammation, atherosclerosis and tumor angiogenesis. The barrier function of endothelial monolayers results from an equilibrium between adhesive strengths which connect ECs to each other via a complex set of junctional proteins and to the extracellular matrix (ECM) proteins via integrins, and contractile forces. Generation of contractile forces within endothelial cells can open intercellular gaps, and thus alter the barrier properties of the monolayer. Indeed, earlier reports have clearly established direct relationships between increased permeability and endothelial contraction leading to cell retraction [2 for review]. Endothelial contraction is associated with an extensive rearrangement of actin microfilaments from a circumferential ring to stress fibres composed of bundles of polymerized actin and myosin filaments [3]. It is now well-recognized that vascular permeability is directly controlled by cytoskeleton rearrangements involving the formation of stress fibres.

On the other hand, increasing evidence suggests that lipid raft and caveolae membrane domains play an important role in the regulation of membrane-cytoskeleton interactions [4]. Several cytoskeleton modulators such as phosphatidylinositol 4,5-bisphosphate (PI4,5P2) or Rho GTPases, and cytoskeletal proteins such as actin and vimentin are associated with rafts [5]. In epithelial cells, the structural protein of tight junctions occludin, and the peripheral membrane protein ZO-1 that links tight junctions to actin cytoskeleton, have been found in the detergent-insoluble fractions constituting raft microdomains whereas other transmembrane proteins such as E-cadherin and beta-1 integrin were not enriched in these structures. In addition, part of occludin pool co-immunoprecipitated with caveolin-1 [6]. Interestingly, phospholipase D (PLD) which is also involved in the regulation of cytoskeleton dynamics [7] has been described as associated to lipid rafts [8]. This enzyme which hydrolyzes phosphatidylcholine to phosphatidic acid (PA) and choline exists as two isoforms. Either PLD1 or PLD2, or both isoenzymes have been found in raft domains depending on the type of cell considered. Thus, Yoon et al. [9] have reported the presence of both PLD1 and PLD2 in

the caveolin-1 enriched fractions isolated from human umbilical vein endothelial cells (HUVECs), whereas Cho et al. [10] only detected PLD2.

Most vasoactive agents which have been shown to induce endothelial permeability [2] are able to stimulate endothelial phospholipase D (PLD). Thus, thrombin treatment of HUVECs potently increases the PLD activity in a time- and dose-dependent fashion [11]. Similarly, histamine has been shown to dose-dependently increase the PLD activity of human aortic endothelial cells [12] and bradykinin proved to be an effective PLD activator in bovine pulmonary aortic endothelial cells [13]. Reactive oxygen species (ROS) generated in the vasculature by activated neutrophils or vascular cells have also been implicated in increased endothelium permeability leading to barrier dysfunction. Interestingly, ROS have also been shown to stimulate PLD activity in several cell types including endothelial cells [14,15].

A role for PLD and its product PA has been postulated in the regulation of actin cytoskeleton. The first observations that exogenous PA or lysophosphatidic acid (LPA)-induced PLD activation induced actin polymerisation were made by Exton's group in HC9 fibroblasts [16,17]. The fact that LPA-induced PA generation and stress fibre formation were both inhibited by 1-butanol, and not by 2-butanol, suggested that PLD can control cytoskeletal reorganization. Similar results were obtained later by Cross et al. [18] using porcine aortic endothelial cells and by Porcelli et al. [19] in human airway epithelial cells. Partial inactivation of PLD1 by stable expression of a dominant negative mutant for rPLD1 markedly reduced LPA effects on both PLD activation and stress fibre formation [20]. At variance with the above results Su et al. [21] reported that PLD1 depletion of HeLa cells by shRNA or tetracycline-induced overexpression of PLD1 in CHO cells did not alter the number of spontaneously formed stress fibres. However, the authors did not examine the possible role of PLD2.

To test the hypothesis that one or the other PLD isoform is an important regulator of endothelial permeability we examined the influence of changes in PLD expression or changes in intracellular PA levels on endothelial permeability and actin cytoskeleton organization, using a HUV-EC cell line. Our results show that enhancement of intracellular PA increases endothelial permeability and that PLD2 is more specifically involved in the regulation of basal endothelial permeability presumably due to its preferential localization into lipid rafts.

Mechanistically, our observations suggest that PLD2 dependent increased endothelial permeability is linked to both PA-dependent cytoskeleton rearrangement and activation of the Raf-MEK-ERK1/2 signaling pathway which negatively regulates the expression level of occludin.

2. Materials and methods

2.1. Materials

Triton X-100 was from Pierce. Silica Gel G60 TLC plates were from VWR International (Fontenay sous-Bois, France). [^{3}H]-palmitic acid was from Perkin Elmer Life Sciences. [^{3}H]5'-AMP (specific activity 722 GBq/mmol), MP Hyperfilm, ECL were from GE Healthcare Life Sciences (Orsay, France). HRP-conjugated anti-mouse IgG antibody was from Jackson Immunoresearch Laboratories (Soham, UK). Bradford protein assay and HRP-conjugated anti rabbit IgG antibody were from Bio-Rad (Marnes-La-Coquette, France).Anti-occludin antibody was from Zymed (Invitrogen, Cergy Pontoise, France). Anti pERK (sc-7383) antibody (Santa Cruz Biotechnology), compounds U-0126 and PD98059 were from TEBU (Le Perray-en Yvelines, France). Immobilon P membranes were from Millipore (St Quentin Yvelines, France). Endothelial cell growth factor, fibronectin, phospholipase D from *Streptomyces chromofuscus*, L-α dioctanoyl phosphatidic acid and egg yolk phosphatidic acid (sodium salts), L-α-oleyl-lysophosphatidic acid, sphingosine-1 phosphate (S1P), filipin, raf-1 inhibitor GW 5074, anti α-tubulin monoclonal antibody, horseradish peroxydase, PLD1 and PLD2 siRNA were from Sigma-Aldrich (L'Isle d'Abeau, France). Negative control siRNA were from Eurogentec (Anger, France). PLD1- and PLD2-specific polyclonal antibodies were kindly provided by Dr S. Bourgoin (Laval University, Canada).

2.2. Cell culture

Human Umbilical Vein Endothelial Cells (HUV-EC, CRL-1730) and Human Embryonic Kidney cells (HEK 293) were obtained from American Type Culture Collection (Rockville,

MD). HUV-EC cells were maintained in Ham's F12K medium containing 10% (vol/vol) foetal calf serum, 2.5g/l sodium bicarbonate, 100 U/ml penicillin, 100 µg/ml streptomycin and 1ml/100ml culture medium of endothelial cell growth factor, in 5% CO_2 at 37°C in a humidified incubator. Treatments were carried out on 100% confluent cells. For adenoviral amplification, HEK 293 cells were maintained in DMEM containing 5% (vol/vol) foetal calf serum, 100 U/ml penicillin, and 100 µg/ml streptomycin.

2.3. PLD assay in intact HUV-EC

PLD activity was determined on the basis of its transphosphatidylation activity. Cells were labelled in serum-free medium containing 2 µCi/ml [^{3}H]palmitic acid for 2 h at 37°C. Cells were then washed twice with ice-cold PBS and treated for the indicated times with LPA and S1P. Butan-1-ol (1% final concentration) was added 30 min before the end of each treatment. Cells were then collected and lipids extracted by the method of Bligh and Dyer [22] in the presence of 50 µM butylhydroxylated toluene. Phosphatidylbutanol was separated by bidimensional TLC using chloroform/methanol/28% ammonia (65:35:5.5, by volume) for the first migration, and ethyl acetate/isooctane/acetic acid (9:5:2, by volume) for migration in the second dimension. TLC plates were then stained with Coomassie Brilliant Blue R, phosphatidylbutanol spots were scraped off and the radioactivity determined by liquid scintillation counting. Radioactivity associated with phosphatidylbutanol was expressed as percentage of total phospholipid radioactivity.

2.4. Measurement of paracellular permeability

The HRP flux which reflects the paracellular permeability was measured according to the procedure of Hirase et al. [23] with slight modifications. Briefly, HUV-EC were seeded onto 0.4 µm polycarbonate Transwell filters (BD Falcon) coated with 5 µg/ml fibronectin. Confluent cells were incubated in serum free medium for 2-3 h before treatment. Resistance of HUV-EC monolayers was measured using Milicell Electrical Resitance System (Millipore) at the beginning of the experiments to verify that the permeability was equivalent for each

transwell system. Then, cells were incubated with the different agonists, in presence or absence of inhibitors, for the indicated periods of time. HRP dissolved in sterile water to give a final concentration of 35 µM was added simultaneously with drugs in the upper compartment at the beginning of experiment. The upper and lower chambers contained 1.5 ml and 3 ml of serum-free medium, respectively (6-well system) or 1 ml and 2 ml (12-well system). 30 min, 1 h, 2 h, 4 h and 24 h after HRP addition, 100 µl of medium was collected from the lower chambers. The HRP content was evaluated spectrophotometrically by assaying peroxidase activity in buffer containing 3.3 mM guaiacol, 180 mM Na_2HPO_4 and 4.7 mM H_2O_2 using 96-well plates. Absorbance was measured at 470 nm. Each experiment was performed in quadruplicate.

2.5. PLD's adenoviral construction and virus production

Recombinant adenoviral genomes carrying the cDNA of interest (hPLD1, hPLD2 or GFP) were generated by homologous recombination as previously described [24]. Briefly, $CaCl_2$ competent *E. coli* BJ5183 was co-transformed with 200 ng of SwaI-linearized VmAdcDNA3 plasmid and 600 ng linearized pCDNA3hPLD1 or pCDNA3hPLD2. The hPLD1b and hPLD2 cDNAs in pCDNA3 plasmids were provided by Dr M. Record (INSERM U563, Toulouse, France). Recombinants were screened by PCR with the following set of primers: A) 5'-GACGGATGTGGCAAAAGTGA annealing to the leftmost part of the adenoviral genome; and B) 5'-ATGGGGTGGAGACTTGGAAATC annealing to portion of the CMV promoter, which is brought in by homologous recombination. Positive clones were further analyzed by restriction analysis. Positive recombinants were amplified in *E.coli* XL-1 blue, digested with PacI and finally transfected by the calcium phosphate method in HEK293 cells. Cytopathic effect due to virus production was observed 8–10 days after transfection. Adenoviruses were extracted by three freeze/thaw cycles and stored in PBS, 10% (vol/vol) glycerol at -20°C. Viral titer of stocks was more than 10^8 plaque-forming units/ml. Infections were performed at the M.O.I. (multiplicity of infection) 100 in complete medium. After 12 h of incubation in the presence of viral particles, the medium was changed and cells were cultured for 24–72 h. Under these conditions, 75% of the cells expressed GFP.

2.6. Short interfering RNA (siRNA) synthesis and transfection

SiRNA for PLD1 (hPLD1 target sequence: AAGTTAAGAGGAAATTCAAGC) and siRNA for PLD2 (hPLD2 target sequence: GACACAAAGTCTTGATGAG) were designed according to Fang et al. [25] and Powner et al. [26], respectively. A siRNA without sequence similarity with any known mammalian gene was used as a negative control. Transfection of siRNA was performed using Xtreme Gene reagent (Roche) with 50 nM siRNA in antibiotic-free medium. The cells were kept for 12 h in this medium and then shifted to complete culture medium for 48 h before treatment.

2.7. Reverse transcriptase and real time PCR

Total RNA was isolated from HUV-EC using Trizol Reagent (Invitrogen) according to the manufacturer's protocol. After quantification, 200 ng of total RNA was reverse transcribed in presence of 100 U Superscript II (Invitrogen) using random hexamers and oligo(dT). Real-time PCR was performed with Fast Start DNA Master SYBR Green kit using a Light-Cycler. Specific sense and anti-sense primers used for amplification were as follows :
occludin: sense: 5'-ATGTGTCTGCAGGCACACAGG; antisense: 5'-AGGCTGCCTGAAGTCATCCAC; PLD1: sense: GGCCATCAAGATAGCCAAGG; antisense: AAGCGTGACAGTGAAATGG; PLD2: sense: ACAGACTGGTGGTTGAGTCC; antisense: AGCCACTGTTGATGCCCAAG. Data were normalized to the TATA binding protein (TBP) and ribosomal protein (RPLPO) housekeeping gene transcripts. Data were analyzed using LightCycler software (Roche Diagnostics).

2.8. Isolation and characterization of lipids rafts from HUV-EC

Lipids rafts were isolated according to the procedure of Diaz et al. [27] based on the insolubility of these structures in cold non-ionic detergent, with slight modifications. Briefly, 20-25 x 10^6 HUV-EC-C were homogenized in 1 ml of ice-cold lysis buffer (25 mM Tris, pH

7.5, 150 mM NaCl, 5 mM EDTA) supplemented with a mixture of protease inhibitors (protease inhibitor mixture Sigma). After centrifugation at 800 g at 4 °C for 10 min, the post-nuclear supernatant was incubated with Triton X-100 at a final concentration of 1% for 1 h at 4 °C. The lysate was then adjusted to 1.3 M sucrose by the addition of an equal volume of 2.6 M sucrose and placed at the bottom of an ultracentrifuge tube, and a step sucrose gradient (0.2–0.9 M with 0.1 M steps, 1 ml each) was placed on top. It was centrifuged at 200,000g for 16 h in an SW41 rotor (Kontron) at 4 °C. One-ml fractions were recovered from the bottom to the top of the gradient. The sucrose concentration of each fraction was determined with a Brix refractometer (Merck). Aliquots were immediately used for 5'-nucleotidase assays, and the remaining was stored at -20°C until analyses.

Proteins were determined by the method of Shaffner and Weissmann [28] using BSA as a standard. Gradient protein recovery relative to total proteins in the post nuclear supernatant varied from 60 to 91%.

5'-Nucleotidase activity of the glycosylphosphatidylinositol-anchored CD73, used as a marker of lipid rafts, was assayed as described by Gentry and Olsson [29] with slight modifications. Aliquots of the gradient fractions were incubated with 1 μM [^{3}H]5'-AMP in 1 ml of reaction mixture containing 60 mM Tris, pH 7.4, 1 μM erythro-9-(2-hydroxy-3-nonyl)adenine to inhibit endogenous adenosine deaminase, 20,000 cpm [^{14}C]adenosine as an internal standard, with or without 25 μM adenosine 5'-(α, β-methylene) diphosphate (AMPCP) to inhibit 5'-nucleotidase activity, for 30 min at 37 °C. The incubation was terminated by addition of 200 μl of 5% ZnSO4 and 200 μl of 0.3 M Ba(OH)2. After centrifugation, the radioactivity of supernatant containing [^{3}H]adenosine was measured by liquid scintillation counting. 5'-nucleotidase activity obtained by difference between values with and without AMPCP was expressed as nmol of 5'-AMP hydrolysed per min per mg of proteins.

Ganglioside M1 (GM1) was quantified on dot blots according to Diaz et al. [27]. Briefly, 20 μl of each gradient fraction were dotted onto Immobilon using a Hybri-Dot Manifold apparatus (Bethesda). Membranes were rinsed with distilled water and blocked with 5% bovine serum albumin in TBS-T for 2 h. After three 10-min washes with TBS-T, membranes were incubated with horseradish peroxidase-conjugated cholera toxin in TBS-T containing

1% bovine serum albumin for 90 min and then rinsed 7 times with TBS-T and developed with the ECL reagent. The luminograms were quantified using cooled digital CCD camera system (ImageMaster VDS-CL, GE Healthcare, France) and Image Quant software. Results are expressed relative to the sum of the intensity of spots present in the different gradient fractions, taken as 100.

Cholesterol was determined enzymatically using a commercial assay kit (Sigma) according to the manufacturer's recommendations.

2.9. Western blotting experiments

PLD. Cells were homogenized in 20 mM Tris/HCl pH 7.6 buffer containing 100 mM NaCl, 1% Triton, and protease inhibitors cocktail. Cell lysates were mixed with Laemmli buffer supplemented with 2 M urea, boiled for precisely 1 min, and separated on 8% SDS polyacrylamide gel including 4 M urea. The blots were probed with PLD1- and PLD2-specific polyclonal antibodies kindly provided by Dr S. Bourgoin (Laval University, Canada), diluted 1:2000. Immunoblots were revealed with the ECL detection system and x-ray film autoradiography. After stripping, the membranes were reprobed with an anti-α-tubulin monoclonal antibody for normalization. Bands were then quantified using cooled digital CCD camera system and Image Quant software. Protein concentrations were routinely determined by the Bradford method [30] using BSA as a standard.

Gradient fractions. 30 µl of gradient fractions were mixed with Laemmli buffer, boiled for 5 min, separated on SDS PAGE and electrotransferred on Immobilon P membrane. For immunodetection the following primary antibodies were used: caveolin-1 (dilution 1/750), occludin and E-cadherin (1 µg/ml). The anti-mouse secondary antibody was diluted 1/10000; the anti-rabbit secondary antibody was diluted 1/5000. Immunoreactive proteins were visualized using ECL detection kit and x-ray film autoradiography. For PLD1 and PLD2 Western blotting, proteins from 600 µl of each fraction were precipitated with ice-cold acetone, and pellets were dissolved in 30µl of Laemmli buffer containing 4 M urea. Bands were then quantified using cooled digital CCD camera system and Image Quant software.

Results are expressed relative to the sum of the intensity of the corresponding bands present in the different gradient fractions, taken as 100.

2.10. Fluorescence staining of actin filaments

HUV-EC cells stimulated with the different agonists or adenovirus infected HUV-EC were washed, fixed in 3.7% formaldehyde for 20 min at 4°C, permeabilized with 0.1% Triton or 50 µg/ml digitonin for 10 min at room temperature and aspecific labelling was blocked in 1% or 0.1% BSA for 20 min. F-actin was stained with rhodamine-conjugated phalloidin and labelled cells were examined by fluorescence microscopy with an Axiovert 200 microscope, an objective LDA-plan, 20x/0.30 PHI ∞/40, an Axiocam MRm camera. F-actin fluorescence was quantified with the Axiovision 4.1 image acquisition software (Carl Zeiss, Göttingen, Germany), by determination of the mean density of randomly selected individual cells, with identical settings for image acquisition from the various preparations.

2.11. *Immunoflurescence staining of occludin*

Untreated or infected cells grown on 12-well plastic plates were preextracted with 0.1% Triton X-100 in 100 mM KCl, 3 mM MgCl2, 1 mM CaCl2, 200 mM sucrose, and 10 mM Hepes (pH 7.1) for 1 min on ice. After 2 PBS washes, cells were fixed with 3.7% paraformaldehyde for 20 min and subsequently permeabilized with 0.05% Triton X-100 for 3 min. The fixed cells were blocked for 20 min in PBS containing 1% BSA. Primary anti-occludin antibody was diluted (1/25) in the same solution and incubated with the cells overnight. After washing, cells were incubated with Alexa-fluor 546 coupled secondary mouse antibody for 1h. Labelled cells were examined by fluorescence microscopy.

2.10. Statistical analysis

Data expressed as means ± SEM were analyzed by one-way ANOVA and means were compared by a protected *t*-test. $P < 0.05$ was considered significant.

3. Results

3.1. PLD agonists increase endothelial permeability

We first evaluated the effects of physiological mediators of endothelial function on PLD activity and endothelial permeability of HUV-EC monolayers. In agreement with previous reports [18,31] both LPA and sphingosine 1-phosphate (S1P) increased the PLD activity of HUV-EC monolayers, with maximal activation being obtained after 5 min of treatment. Although S1P effect was twice that of LPA at early time points, it declined very quickly. After 30 min of treatment S1P-stimulated PLD activity returned to basal level whereas LPA effect was maintained throughout this period and declined thereafter (Fig. 1A). LPA also induced a time-dependent increase in endothelial permeability for horseradish peroxidase (HRP) as compared with HRP passage through untreated cell monolayers (taken as 1 at each time point). The LPA-induced increase in permeability lasted for several hours, a maximal 1.7-fold increase being observed at 4 h (Fig. 1B). After 24 h the permeability of LPA-treated monolayers did not differ significantly from that of untreated control monolayers. S1P treatment of HUV-EC also increased HRP passage across monolayers. As observed for PLD activity, S1P effect was maximal earlier than LPA effect (1 h vs 4 h) and started to decline thereafter (Fig. 1C).

3.2. Increased level of intracellular PA increases endothelial permeability

To explore further the potential role of PLD in the control of endothelial permeability, we examined the effects of several agents known to increase endogenous PA [14]. The addition of a bacterial PLD from *Streptomyces chromofuscus* to HUV-EC monolayers maximally increased HRP flux after 1 to 2 h of treatment, suggesting that a certain lag-time is necessary to achieve increase of PA level (Fig. 2A). In contrast, propranolol a well-known inhibitor of PA hydrolase which has been shown to induce endogenous PA accumulation [32,33] markedly and rapidly increased endothelial permeability, maximal effect being already

obtained after 30 min of treatment (Fig. 2B). Finally, addition of the cell permeant di-C8-PA induced a gradual increase in permeability which peaked after 2 h and declined thereafter (Fig. 2C). Similar effects were obtained with PA originating from egg yolk (not shown).

3.3. PLD2 but not PLD1 overexpression increases basal endothelial permeability

Results of the above experiments indicate that enhancing endogenous PA level either through PLD activation or inhibition of PA degradation markedly increased endothelial permeability. To investigate further which PLD isoform is more specifically involved in the control of endothelial paracellular permeability, HUV-EC were infected with adenovirus constructs containing the cDNA of hPLD1b, or hPLD2, or GFP for control. Western blots in Fig. 3A show that the expression level of both PLD1 and PLD2 was markedly increased in infected cells as compared with non infected cells or cells infected with control GFP adenovirus. HRP flux across infected HUV-EC monolayers was measured 72 h post infection. HUV-EC infected with PLD2 adenovirus exhibited a sustained increase of permeability as compared to cells infected with control GFP adenovirus. In contrast, HRP flux across PLD1 adenovirus infected HUV-EC was not significantly different from that observed with control GFP adenovirus infected cells (Fig. 3B).

3.4. Downregulation of PLD1 and PLD2 differently affects basal and stimulated endothelial permeability

Given the lack of isoform specific PLD inhibitors, we examined the effect of PLD1 and PLD2 knockdown by means of specific siRNA on endothelial permeability. As shown in Fig 4A, both PLD1 and PLD2 siRNA reduced the level of the corresponding protein by around 70 % without affecting the other isoform. Interestingly, only PLD2 silencing was able to reduce basal HRP flux across HUV-EC monolayers confirming the prevalent role of PLD2 over PLD1 as a regulator of basal endothelial permeability (Fig. 4B). PLD2 silencing also suppressed LPA-induced short-term (30 min) increase in permeability, whereas PLD1 silencing did not (Fig. 4C). In contrast, both PLD1 and PLD2 silencing counteracted the

stimulatory effect of LPA on HRP flux measured after 2h of treatment, as compared with LPA effect on cells transfected with control siRNA (Fig. 4D).

3.5. Increased level of intracellular PA induces actin stress fibre formation

The stimulation of HUV-EC by both PLD agonists LPA and S1P resulted in a rapid rearrangement of the actin network into thick bundles of stress fibres transversing the cell. Fibre formation was detected within a few minutes (not shown) and reached a maximum by 15-30 min (Fig. 5). They started to disappear after 30 min for S1P and 1 h for LPA (not shown). These observations suggest that actin reorganization precedes cell contraction and cell junction disorganization, and as a consequence, increased endothelial permeability (Figs. 1B and C). PLD agonists-stimulated stress fibre formation was inhibited by the primary alcohol 1-butanol, which decreases endogenous PA, but not by 2-butanol, an inactive isomer (not shown). The treatment of HUV-EC by diC8-PA or propranolol which increases endogenous PA level through inhibition of PA hydrolase [32,33] also induced actin stress fibre formation. Thus, 45 ± 9 and 51 ± 6 % of cells treated with 50 µM diC8-PA or 25 µM propranolol, respectively, were stress fibre positive whereas only 6 ± 6 % of untreated control cells showed stress fibres. To investigate further the possible relationships between stress fibre formation and increased endothelial permeability we examined the effects of PLD overexpression on the reorganization of actin cytoskeleton. As shown in Figs. 5B and C, the percentage of stress fibre positive cells was significantly increased in cells infected with PLD2-adenovirus (36.7 ± 3.7 %) as compared with non-infected cells (12.2 ± 0.9 %) or cells infected with GFP-adenovirus (11.3 ± 1.8 %). In contrast, in cells infected with PLD1-adenovirus, the percentage of stress fibre positive cells (18.8 ± 1.8 %) did not significantly differ from those measured in non-infected and GFP-adenovirus infected cells (Figs. 5B and C). Interestingly, in the same experimental conditions, only PLD2 overexpression was able to significantly increase endothelial permeability (Fig. 3B). To more thoroughly investigate the respective role of the two PLD isoforms in LPA-induced stress fibre formation, we examined actin cytoskeleton response to LPA in cells transfected with control siRNA and with PLD1- or PLD2-siRNA. Data shown in Figs. 5D and E indicate that PLD2 silencing totally

suppressed the rapid formation of stress fibres in response to LPA whereas PLD1 silencing did not prevent actin reorganization induced by LPA.

3.6. A substantial part of PLD2 is located to the detergent insoluble microdomains (lipid rafts) of HUV-EC

Lipid rafts were isolated from HUV-EC by fractionation of Triton X-100 treated cell lysates on a discontinuous sucrose density gradient. The low-density fractions containing 15 to 21 % sucrose contained specific markers of lipid rafts. Thus, about 53% of the enzymatic activity of 5'-nucleotidase, a glycosylphosphatidylinositol (GPI)-anchored protein [5] were recovered in the gradient fractions 6 to 8, which contained less than 4% of total proteins (Fig. 6A). These low-density fractions were also enriched in cholesterol (about 30% of total) (Fig. 6B) and contained most part (79%) of the ganglioside GM1 (Fig. 6C). They were further characterized by Western blotting experiments. As shown in Fig. 6D, the gradient fractions 6 to 8 were markedly enriched in caveolin-1 (57.2 ± 5.8 %, *N*=3) and also contained part of the junctional protein occludin which has also been found in the detergent insoluble fractions of T84 epithelial cells [6]. In contrast, E-cadherin and claudin-1 were not preferentially associated with the raft fractions (not shown). Interestingly, a substantial part of PLD2 protein (42.6 ± 1.8 %, *N*=3) was present in the low-density fractions of the gradient, whereas only 16.1 ± 4.2% (*N*=3) of PLD1 protein were recovered in these raft fractions (Fig. 6D).

3.7. Disruption of lipid rafts inhibits LPA effects on stress fibre formation and endothelial permeability

To determine the importance of membrane raft integrity for stress fibre formation and increased endothelial permeability, HUV-EC were treated with filipin (2 µg/ml), a cholesterol binding toxin, for 30 min before LPA activation. LPA stimulated actin reorganization into thick stress fibres (Fig. 5A, and Fig. 7A) and induced the formation of paracellular gaps in the monolayer. Filipin pretreatment significantly prevented both of these effects (Figs. 7A, and B). Indeed, only 12 ± 2 % of cells pretreated with filipin became stress fibre positive upon

LPA activation, whereas this percentage reached 32 ± 4 % in the absence of filipin. In addition filipin also prevented LPA-induced increase in endothelial permeability (Fig. 7C). Altogether, these results indicate that raft integrity is necessary for maintaining actin dynamics, and suggest that PLD2 effects on stress fibre formation and endothelial permeability that we observed in the present study might be related to the preferential location of the enzyme in raft domains.

3.8. PLD2 but not PLD1 overexpression downregulates occludin expression

Occludin plays a critical role in regulating the barrier function of endothelial monolayers. Indeed, the loss of occludin at endothelial junctions induced by VEGF treatment has been associated with an increased permeability of endothelial monolayers through a signaling pathway involving mitogen-activated protein (MAP) kinases [34]. Given the results of the present study showing that PLD2 overexpression increased HRP flux through HUV-EC monolayers (Fig. 3), we then compared the level of occudin expression in cells infected by the different adenovirus constructs. Western blotting experiments shown in Figs. 8A and B, indicate that occludin level was significantly decreased in cells overexpressing PLD2, as compared with non-infected cells or cells infected by the other adenovirus constructs. Such downregulation was accompanied by a loss of occludin protein expression at cell periphery (Fig. 8C) and was confirmed by a significant decrease of occludin mRNA levels (Fig. 8D). Concomitantly with changes in occludin expression, an increased level of phosphorylated ERK (Figs. 8E and F) was also observed, whereas the level of phosphorylated p38 MAP kinase was not altered (Figs. 8G and H). In contrast, PLD1 overexpression did not induce significant changes in occludin expression level or ERK phosphorylation. These results show that PLD2 overexpression downregulates occludin and stimulates the MEK/ERK pathway, thus suggesting a possible link between both events, as it has been demonstrated in epithelial cells [35]. Indeed, transient transfection of Pa-4 epithelial cells with a constitutively active form of MEK1 drastically reduced occludin mRNA level, such downregulation being blocked by the MEK inhibitor PD98059 [35].

3.9. Activation of ERK1/2 by Raf-1 is required for PA-mediated increase of endothelial permeability

The MAP kinase pathway is known to mediate an elevation of endothelial permeability [36]. To examine whether the MAP kinase cascade was involved in PA induced hyperpermeability, HUV-EC were pretreated with the MEK inhibitors PD98059 and U-0126 before stimulation of cells with LPA. These compounds have been shown to prevent the activation of ERK1/2 and the subsequent phosphorylation of ERK1/2 substrates both in acellular systems and in intact cells [37,38)]. As shown in Fig. 9A, pretreatment of HUV-EC with the MEK inhibitors significantly reduced the elevation of permeability induced by LPA. Furthermore, Raf-1, a serine/threonine kinase which directly activates MEK and the MAP kinase cascade is a well-known target of PA. Raf-1 is activated through translocation to PA-enriched domains of plasma membrane driven by the ligation of PA to a specific domain of the protein, and interaction with Ras [39]. To examine whether Raf-1 was involved in the PA-induced hyperpermeability, we used a selective Raf-1 kinase inhibitor, GW-5074 [40]. GW-5074 significantly attenuated LPA and PA-induced hyperpermeability (Figs. 9B and C). Moreover, GW-5074 suppressed hyperpermeability induced by PLD2 overexpression without altering the permeability of PLD1- or GFP-overexpressing cells (Fig. 9D). Western blotting experiments show that ERK1/2 was activated by PA and LPA (Figs. 9E-H). Pretreatment of HUV-EC for 30 min with 100 nM GW-5074 reduced LPA and PA-induced ERK-1/2 phosphorylation (Figs. 9E-H). Altogether, these data show that Raf and ERK1/2 are downstream effectors of PA and are necessary for PA induced-hyperpermeability.

4. Discussion

The barrier function of vascular endothelium is a highly regulated process involving intricate signaling cascades [2]. Any dysfunction of this barrier may lead to pathological situations including inflammation and atherosclerosis. PLD and PLD-generated PA have been implicated in the increased permeability induced by ROS and pro-oxidant compounds, especially in bovine pulmonary arteries [14]. However the signaling pathways downstream of PLD leading to endothelium permeability changes have not been clearly defined. In the present study we used a variety of approaches to increase the intracellular PA and to establish potential links between elevation of PA level, cytoskeleton rearrangements, tight junction disturbance and increased endothelial permeability. We first used two agonists of lysophospholipid receptors, LPA and S1P [41], both of them having been shown to stimulate PLD activity in some types of cells. Indeed, LPA has been described as a PLD activator in fibroblasts [16], endothelial cells [18], epithelial cells [19], prostate cancer cells [42] or human neutrophils [43], whereas S1P-induced PLD activation has been reported in fibroblasts [44], bronchial epithelial cells [45] or pulmonary endothelial cells [46]. Both LPA and S1P have been shown to either increase or decrease monolayer permeability depending on the endothelial cell type considered. There are four LPA receptors and five S1P receptors identified in mammals to date [41]. They are coupled to a variety of downstream signaling cascades through different classes of G proteins including Gi, Gq, $G_{12/13}$. Whereas coupling through $G_{12/13}$ activates exclusively the RhoA pathway leading to stress fibre formation and increased permeability due to cell retraction and intercellular gap formation, coupling through Gi activates both Rac and RhoA. Unlike RhoA, Rac activation induces cortical actin formation, assembly of adherens junctions and improves endothelial barrier function [47,48]. Thus, the final outcome of LPA and S1P action on vascular permeability may be determined by the balance between RhoA and Rac activation depending on the type of endothelial cell considered. In the HUV-EC line used in the present study both LPA and S1P stimulated PLD activity, induced transient stress fibre formation and increased endothelial permeability, thus suggesting the prevalence of RhoA-dependent signaling pathways. Besides LPA and S1P, we used different treatments to increase PA intracellular level, namely exogenous dioctanoyl PA,

propranolol and bacterial scPLD. Dioctanoyl PA, a cell permeant compound, has been shown to exert effects similar to those obtained with PLD-generated PA in various cell models [49]. Propranolol, a well-known inhibitor of PA phosphohydrolase has been shown to increase PA levels in many types of intact cells including smooth muscle cells [50] or L6 myoblasts [33]. Finally, PLD from *Streptomyces chromofuscus* has been widely used to induce PA synthesis in membranes of living cells to mimic the effects of endogenous mammalian PLD. In addition, this bacterial enzyme also possesses lysoPLD activity and is able to catalyze the synthesis of LPA from LPC [51], both activities leading to increased PA level either directly or through LPA-induced endogenous PLD activation. The three agents used to enhance intracellular PA level increased HRP flux through endothelial monolayers and induced the formation of stress fibre bundles. The effect of PLD activation on cytoskeleton reorganization has been proposed to be due to the ability of PA to bind and activate the PI4P 5-kinase leading to an increased level of PI4,5P2 [52]. PI4,5P2 is known to interact with several actin regulating proteins such as profilin, gelsolin or cofilin thus promoting the formation of actin bundles [53].

It is well-recognized that actin polymerization is a Rho-dependent process [54]. One of the best characterized targets of RhoA is the p160 Rho kinase which phosphorylates the myosin light chains (MLC) directly and also inhibits MLC dephosphorylation. The resulting increase of MLC phosphorylation level contributes to actin stress fibre formation and increased actomyosin contractility [54]. RhoA is also a well-known PLD activator [8]. Thus, it is conceivable that the RhoA-stimulated PA synthesis also contributes to stress fibre accumulation. However, RhoA selectively activates the PLD1 isoform whereas PLD2 is not sensitive to RhoA regulation [8]. In our cell model, overexpressing PLD2 increased basal permeability (Fig. 3B), possibly due to the formation of stable stress fibres (Fig. 5B), and also through decreased expression of occludin and disturbance of intercellular junctions resulting from occludin loss (Fig. 8C). PLD2 thus seems to regulate basal endothelial permeability, as confirmed by the effect of PLD2 depletion which reduced basal permeability (Fig. 4B). On the contrary, based on overexpression experiment (Fig. 3B), PLD1 does not seem to regulate basal endothelial permeability. This might be linked with the fact that overexpression of PLD1 induces by itself only a weak formation of stable stress fibres (Fig. 5B), and does not

influence occludin expression and pericellular location (Fig. 8C). This is in agreement with the inability of PLD1 depletion to reduce basal permeability (Fig. 4B).

It must be noticed that PLD1 activity under basal conditions, due to its much lower specific activity [55] and lower level of expression in HUV-EC cells (2-fold as evaluated by real time qPCR experiments, results not shown) as compared with PLD2, represents only a minor part of total PLD activity, and might thus play a negligible role. Instead, in LPA-stimulation conditions, PLD1 is likely to be activated [19] in particular via RhoA, and the contribution of PLD1 activity may become important. We indeed observed that PLD2-si RNA had a strong inhibitory effect on basal PLD activity, whereas PLD1-siRNA had no effect. Furthermore, PLD2-siRNA and PLD1-siRNA similarly inhibited LPA-stimulated PLD activity (not shown). Accordingly, PLD1 depletion, as well as PLD2 depletion, decreased the permeability measured after long term (2h) LPA treatment, suggesting that both PLD isoforms are necessary for LPA to increase permeability (Fig. 4D).

Surprisingly, only PLD2 depletion strongly prevented rapid LPA-induced stress fibre formation while PLD1 depletion had no effect (Figs. 5D and E), suggesting that stress fibres play little role in the increase in permeability induced by LPA. However, since the observation of stress fibres was performed after a short treatment by LPA (15 min), whereas the suppression of permeability increase by PLD1- and PLD2-siRNAs was observed after 2 h of LPA treatment (when LPA-induced stress fibres have subsided), it is possible that only the short-term increase in permeability induced by LPA (0.5-1 h, Fig. 1B) was caused by transient stress fibre formation and cell retraction, and is thus dependent on the sole PLD2. In support to this, when permeability was measured after a short treatment by LPA (30 min), only PLD2 depletion significantly affected permeability, PLD1 depletion having no significant effect (Fig. 4C). Instead, the delayed increase in permeability induced by LPA ($\geq$2 h), could be independent of transient stress fibres and necessitate both PLD1 and PLD2. In this regard, it has been claimed by several authors that PLD1 could be regulating PLD2, possibly through the production of PI4,5P2 [56,57]. PLD2 might thus be the key player in endothelial permeability regulation, with PLD1 playing an accessory role. The observation that PLD1 and PLD2 isoforms differently affect basal cell functions has been made in other

cell models. For example, Padron et al. [58] have shown that only PLD2 silencing reduced the recycling of transferrin receptors in HeLa cells, whereas siRNA against PLD1 had no effect.

The difference of effect between PLD1 and PLD2 on endothelial permeability might also be related to their different subcellular localization. Our fractionation experiments showed that the proportion of PLD2 protein present in the low-density fractions of the gradient enriched in specific markers of raft structures and caveolin was about 2.7-fold higher than that of PLD1 (Fig. 6). Interestingly, PLD2 has been described as the only PLD isoform present in lipid microdomains of primary cultured HUVEC [10]. Results of the present study showed that the integrity of raft structures/caveolae is a prerequisite for LPA effect on endothelial permeability. Indeed, pretreatment of HUV-EC with the cholesterol-sequestering agent filipin abrogated both actin stress fibre formation and increased HRP flux induced by LPA activation (Fig. 7). In bovine aortic endothelial cells, the formation of stress fibres induced by thrombin was only dependent on raft integrity because it was suppressed by filipin but not by caveolae disorganization through caveolin depletion [59]. Because cholesterol sequestration alters both membrane rafts and caveolae, we cannot associate LPA effect, and thus PLD activation, to one or the other structure.

Besides cytoskeleton reorganization and cell contraction, interendothelial junctions, and among them tight junctions, represent another major device regulating endothelial permeability [2]. It has been shown that the quality of the endothelial barrier is directly correlated to the level of occludin expression [34]. Furthermore the loss of occludin at endothelial and epithelial junctions appears to result from a Raf-1-dependent activation of MAP kinase signal transduction cascade [60,61]. In the present study, we observed that PLD2 overexpression induced a significant decrease of occludin expression at cell periphery. Downregulation of both occludin protein and mRNA was accompanied by a significant ERK1/2 activation evaluated by the level of phosphorylated ERK1/2 proteins. Unlike ERK1/2, p38 MAP kinase phosphorylation level was not modified by PLD2 overexpression. Because Raf-1 kinase is a well-known target of PA [39], we further investigated whether Raf-1 kinase/MAP kinase were involved in the signaling pathway leading from PLD activation to increased permeability. We showed that the Raf kinase inhibitor GW-5074 was able to drastically reduce hyperpermeability induced by PLD2 overexpression. GW-5074 also

inhibited the PA- and LPA-induced increase in endothelial permeability and ERK1/2 phosphorylation level, suggesting that hyperpermeability resulting from PA accumulation involved the sequential activation of Raf-1 and ERK1/2. It has been recently demonstrated that activation of the Raf/MEK/ERK1/2 pathway induces the upregulation of the transcriptional repressor Slug, which in turn inhibits occludin expression through interaction with the occludin promoter [60]. On the other hand, it is also known that MAP kinase activation can rapidly induce hyperpermeability through occludin displacement from tight-junctions [61]. Thus, we propose that activation of the Raf/MEK/ERK1/2 pathway by increased PA intracellular level has both fast and long term effects on endothelial permeability, through tight-junction regulation .

On the whole, the present results demonstrate the selective role of PLD2 isoform in the control of endothelial permeability, through a mechanism involving both stress fibre formation and contraction, and occludin displacement and downregulation subsequent to PA-mediated activation of Raf-1 and its downstream targets MEK-1 and ERK1/2.

Acknowledgements

This work was supported by INSERM and a grant from ANR (ANR-05-PCOD-019-01).

References

[1] G. Bazzoni, E. Dejana, Endothelial cell-to-cell junctions: molecular organization and role in vascular homeostasis, Physiol. Rev. 84 (2004) 869-901.

[2] D. Mehta, A.B. Malik, Signaling mechanisms regulating endothelial permeability, Physiol. Rev. 86 (2006) 279-367.

[3] M.S. Kolodney, R.B.Wysolmerski, Isometric contraction by fibroblasts and endothelial cells in tissue culture: a quantitative study, J. Cell Biol. 117 (1992) 73-82.

[4] I. Levitan, K.J. Gooch, Lipid rafts in membrane-cytoskeleton interactions and control of cellular biomechanics: Actions of oxLDL, Antioxid. Redox Signal. 9 (2007) 1519-1534.

[5] R.R. Sprenger, D. Speijer, J.W. Back, C.G. De Koster, H. Pannekoek, A.J. Horrevoets, Comparative proteomics of human endothelial cell caveolae and rafts using two-dimensional gel electrophoresis and mass spectrometry, Electrophoresis 25 (2004) 156-172.

[6] **A.** Nusrat, C.A. Parkos, P. Verkade, C.S. Foley, T.W. Liang, W. Innis-Whitehouse, K.K. Eastburn, J.L. Madara, Tight junctions are membrane microdomains, J. Cell Sci. 113 (2000) 1771-1781.

[7] P.A. Oude Weernink, M. López de Jesús, M. Schmidt, Phospholipase D signaling: orchestration by PIP2 and small GTPases, Naunyn-Schmiedeberg's Arch. Pharmacol. 374 (2007) 399-411.

[8] M. McDermott, M.J. Wakelam, A.J. Morris, Phospholipase D, Biochem. Cell. Biol. 82 (2004) 225-253.

[9] M.J. Yoon, C.H. Cho, C.S. Lee, I.H. Jang, S.H. Ryu, G.Y. Koh, Localization of Tie2 and phospholipase D in endothelial caveolae is involved in angiopoietin-1-induced MEK/ERK phosphorylation and migration in endothelial cells, Biochem. Biophys. Res. Commun. 308 (2003) 101-105.

[10] C.H. Cho, C.S. Lee, M. Chang, I.H. Jang, S.J. Kim, I. Hwang, S.H. Ryu, C.O. Lee, G.Y. Koh, Localization of VEGFR-2 and PLD2 in endothelial caveolae is involved in VEGF-induced phosphorylation of MEK and ERK, Am. J. Physiol. Heart Circ. Physiol. 286 (2004) H1881-H1888.

[11] J.G. Garcia, J.W.2nd Fenton, V. Natarajan, Thrombin stimulation of human endothelial cell phospholipase D activity. Regulation by phospholipase C, protein kinase C, and cyclic adenosine 3'5'-monophosphate, Blood 79 (1992) 2056-2067.

[12] Q. Hu, V. Natarajan, R.C. Ziegelstein, Phospholipase D regulates calcium oscillation frequency and nuclear factor-kappaB activity in histamine- stimulated human endothelial cells, Biochem. Biophys. Res. Commun. 292 (2002) 325-332.

[13] T.W. Martin, D.R. Feldman, K.E. Goldstein, J.R. Wagner, Long-term phorbol ester treatment dissociates phospholipase D activation from phosphoinositide hydrolysis and prostacyclin synthesis in endothelial cells stimulated with bradykinin, Biochem. Biophys. Res. Commun. 165 (1989) 319-326.

[14] R. Cummings, N. Parinandi, L. Wang, P. Usatyuk, V. Natarajan, Phospholipase D/phosphatidic acid signal transduction: role and physiological significance in lung, Mol. Cell. Biochem. 234/235 (2002) 99-109.

[15] P.S. Tappia, M.R. Dent, N.S. Dhalla, Oxidative stress and redox regulation of phospholipase D in myocardial disease, Free Radic. Biol. Med. 41 (2006) 349-361.

[16] K.S. Ha, J.H. Exton, Activation of actin polymerization by phosphatidic acid derived from phosphatidylcholine in IIC9 fibroblasts, J. Cell Biol. 123 (1993) 1789-1796.

[17] K.S. Ha, E.J. Yeo, J.H. Exton, Lysophosphatidic acid activation of phosphatidylcholine-hydrolysing phospholipase D and actin polymerization by a pertussis toxin-sensitive mechanism, Biochem. J. 303 (1994) 55-59.

[18] M.J. Cross, S. Roberts, A.J. Ridley, M.N. Hodgkin, A. Stewart, L. Claesson-Welsh, M.J. Wakelam, Stimulation of actin stress fibre formation mediated by activation of phospholipase D, Curr. Biol. 6 (1996) 588-597.

[19] A.M. Porcelli, A. Ghelli, S. Hrelia, M. Rugolo, Phospholipase D stimulation is required for sphingosine-1-phosphate activation of actin stress fibre assembly in human airway epithelial cells, Cell. Signal. 14 (2002) 75-81.

[20] Y. Kam, J.H. Exton, Phospholipase D activity is required for actin stress fiber formation in fibroblasts, Mol. Cell. Biol. 21 (2001) 4055-4066.

[21] W. Su, P. Chardin, M. Yamazaki, Y. Kanaho, G. Du, RhoA-mediated Phospholipase D1 signaling is not required for the formation of stress fibers and focal adhesions, Cell. Signal. 18 (2006) 469-478.

[22] E.G. Bligh, W.J. Dyer, A rapid method of total lipid extraction and purification, Can. J. Med. Sci. 37 (1959) 911-917.

[23] T. Hirase, S. Kawashima, E.Y. Wong, T. Ueyama, Y. Rikitake, S. Tsukita, M. Yokoyama, J.M. Staddon, Regulation of tight junction permeability and occludin phosphorylation by RhoA-p160ROCK-dependent and -independent mechanisms, J. Biol. Chem. 276 (2001) 10423-10431.

[24] C. Chaussade, L. Pirola, S. Bonnafous, F. Blondeau, S. Brenz-Verca, H. Tronchère, F. Portis, S. Rusconi, B. Payrastre, J. Laporte, E. Van Obberghen, Expression of myotubularin by an adenoviral vector demonstrates its function as a

phosphatidylinositol 3-phosphate [PtdIns(3)P] phosphatase in muscle cell lines: involvement of PtdIns(3)P in insulin-stimulated glucose transport, Mol. Endocrinol. 17 (2003) 2448-2460.

[25] Y. Fang, I.H. Park, A.L. Wu, G. Du, P. Huang, M.A. Frohman, S.J. Walker, H.A. Brown, J. Chen, PLD1 regulates mTOR signaling and mediates Cdc42 activation of S6K1, Curr. Biol. 13 (2003) 2037-2044.

[26] D.J. Powner, R.M. Payne, T.R. Pettitt, M.L. Giudici, R.F. Irvine, M.J. Wakelam, Phospholipase D2 stimulates integrin-mediated adhesion via phosphatidylinositol 4-phosphate 5-kinase Igamma b, J. Cell Sci. 118 (2005) 2975-2986.

[27] O. Diaz, A. Berquand, M. Dubois, S. Di Agostino, C. Sette, S. Bourgoin, M. Lagarde, G. Nemoz, A.F. Prigent, The mechanism of docosahexaenoic acid-induced phospholipase D activation in human lymphocytes involves exclusion of the enzyme from lipid rafts, J. Biol. Chem. 277 (2002) 39368-39378.

[28] W. Schaffner, C. Weissmann, A rapid, sensitive, and specific method for the determination of protein in dilute solution, Anal. Biochem. 56 (1973) 502-514.

[29] M.K. Gentry, R.A. Olsson, A simple, specific, radioisotopic assay for 5'-nucleotidase, Anal. Biochem. 64 (1975) 624-627.

[30] M.M. Bradford, A rapid and sensitive method for the quantitation of microgram quantities of protein utilizing the principle of protein-dye binding, Anal. Biochem. 72 (1976) 248-254.

[31] S. Spiegel, S. Milstien, Sphingoid bases and phospholipase D activation, Chem. Phys. Lipids 80 (1996) 27-36.

[32] Z. Kiss, Sphingosine-like stimulatory effects of propranolol on phospholipase D activity in NIH 3T3 fibroblasts, Biochem. Pharmacol. 47 (1994) 1581-1586.

[33] F. Naro, V. Donchenko, S. Minotti, L. Zolla, M. Molinaro, S. Adamo, Role of phospholipase C and D signalling pathways in vasopressin-dependent myogenic differentiation, J. Cell. Physiol. 171 (1997) 34-42.

[34] C.G. Kevil, D.K. Payne, E. Mire, J.S. Alexander, Vascular permeability factor/vascular endothelial cell growth factor-mediated permeability occurs through disorganization of endothelial junctional proteins, J. Biol. Chem. 273 (1998) 15099-15103.

[35] D. Li, R.J. Mrsny, Oncogenic Raf-1 disrupts epithelial tight junctions via downregulation of occludin, J. Cell Biol. 148 (2000) 791-800.

[36] G. Bazzoni, Endothelial tight junctions: permeable barriers of the vessel wall, Thromb. Haemost. 95 (2006) 36-42.

[37] D.T. Dudley, L. Pang, S.J. Decker, A.J. Bridges, A.R. Saltiel, A synthetic inhibitor of the mitogen-activated protein kinase cascade, Proc. Natl. Acad. Sci. U.S.A 92 (1995) 7686–7689.

[38] M.E. Favata, K.Y. Horiuchi, E.J. Manos, A.J. Daulerio, D.A. Stradley, W.S. Feeser, D.E. Van Dyk, W.J. Pitts, R.A. Earl, F. Hobbs, R.A. Copelznd, R.L. Magolda, P.A. Scherle, J.M. Trzaskos, Identification of a novel inhibitor of mitogen-activated protein kinase kinase, J. Biol. Chem. 273 (1998) 18623–18632.

[39] S. Ghosh, J.C. Strum, V.A. Sciorra, L. Daniel, R.M. Bell, Raf-1 kinase possesses distinct binding domains for phosphatidylserine and phosphatidic acid. Phosphatidic acid regulates the translocation of Raf-1 in 12-O-tetradecanoylphorbol-13-acetate-stimulated Madin-Darby canine kidney cells, J. Biol. Chem. 271 (1996) 8472-8480.

[40] K. Lackey, M. Cory, R. Davis, S.V. Frye, P.A. Harris, R.N. Hunter, D.K. Jung, O.B. McDonald, R.W. McNutt, M.R. Peel, R.D. Rutkowske, J.M. Veal, E.R. Wood, The discovery of potent cRaf1 kinase inhibitors, Bioorg. Med. Chem. Lett. 10 (2000) 223-226.

[41] B. Anliker, J. Chun, Lysophospholipid G protein-coupled receptors, J. Biol. Chem. 279 (2004) 20555-20558.

[42] Y. Xie, T.C. Gibbs, Y.V. Mukhin, K.E. Meier, Role for 18:1 lysophosphatidic acid as an autocrine mediator in prostate cancer cells, J. Biol. Chem. 277 (2002) 32516-32526.

[43] J.S. Tou, J.S. Gill, Lysophosphatidic acid increases phosphatidic acid formation, phospholipase D activity and degranulation by human neutrophils, Cell. Signal. 17 (2005) 77-82.

[44] Y. Banno, H. Fujita, Y. Ono, S. Nakashima, Y. Ito, N. Kuzumaki, Y. Nozawa, Differential phospholipase D activation by bradykinin and sphingosine 1-phosphate in NIH 3T3 fibroblasts overexpressing gelsolin, J. Biol. Chem. 274 (1999) 27385-27391.

[45] L. Wang, R. Cummings, P. Usatyuk, A. Morris, K. Irani, V. Natarajan, Involvement of phospholipases D1 and D2 in sphingosine 1-phosphate-induced ERK (extracellular-signal-regulated kinase) activation and interleukin-8 secretion in human bronchial epithelial cells, Biochem. J. 367 (2002) 751-760.

[46] I. Gorshkova, D. He, E. Berdyshev, P. Usatuyk, M. Burns, S. Kalari, Y. Zhao, S. Pendyala, J.G. Garcia, N.J. Pyne, D.N. Brindley, V. Natarajan, Protein kinase C-epsilon regulates sphingosine 1-phosphate-mediated migration of human lung endothelial cells through activation of phospholipase D2, protein kinase C-zeta, and Rac1, J. Biol. Chem. 283 (2008) 11794-11806

[47] W.H. Moolenaar, L.A. van Meeteren, B.N. Giepmans, The ins and outs of lysophosphatidic acid signaling, Bioessays 26 (2004) 870-881.

[48] T. Sanchez, T. Hla, Structural and functional characteristics of S1P receptors, J. Cell. Biochem. 92 (2004) 913-922.

[49] G.M. Jenkins, M.A. Frohman, Phospholipase D: a lipid centric review, Cell. Mol. Life Sci. 62 (2005) 2305-2316.

[50] K.E. Meier, K.C. Gause, A.E. Wisehart-Johnson, A.C. Gore, E.L. Finley, L.G. Jones, C.D. Bradshaw, A.F. McNair, K.M. Ella, Effects of propranolol on phosphatidate phosphohydrolase and mitogen-activated protein kinase activities in A7r5 vascular smooth muscle cells, Cell. Signal. 10 (1998) 415-426.

[51] E. Billon-Denis, Z. Tanfin, P. Robin, Role of lysophosphatidic acid in the regulation of uterine leiomyoma cell proliferation by phospholipase D and autotaxin, J. Lipid Res. 49 (2008) 295-307.

[52] D.R. Jones, M.A. Sanjuan, I. Mérida, Type Ialpha phosphatidylinositol 4-phosphate 5-kinase is a putative target for increased intracellular phosphatidic acid, FEBS Lett 476 (2000) 160-165.

[53] H.L. Yin, P.A. Janmey, Phosphoinositide regulation of the actin cytoskeleton, Annu. Rev. Physiol. 65 (2003) 761-789.

[54] S. Pellegrin, H. Mellor, Actin stress fibres, J. Cell Sci.120 (2007) 3491-3499.

[55] M. McDermott, M. J. Wakelam, A. J. Morris, Phospholipase D. Biochem. Cell Biol. 82 (2004) 225-253.

[56] D.A. Foster, L. Xu, Phospholipase D in cell proliferation and cancer. Mol. Cancer Res. 1 (2003) 789-800.

[57] W.S. Choi, Y.M. Kim, C. Combs, M.A. Frohman, M.A. Beaven, Phospholipases D1 and D2 regulate different phases of exocytosis in mast cells, J. Immunol. 168 (2002) 5682-5689.

[58] D. Padron, R.D. Tall, M.C. Roth, Phospholipase D2 is required for efficient endocytic recycling of transferrin receptors, Mol. Biol. Cell 17 (2006) 598-606.

[59] M. Carlile-Klusacek, V. Rizzo, Endothelial cytoskeletal reorganization in response to PAR1 stimulation is mediated by membrane rafts but not caveolae, Am. J. Physiol. Heart Circ. Physiol. 293 (2007) H366-H375

[60] Z. Wang, P. Wade, K.J. Mandell, A. Akyildiz, C.A. Parkos, R.J. Mrsny, A. Nusrat, Raf 1 represses expression of the tight junction protein occludin via activation of the zinc-finger transcription factor slug, Oncogene 26 (2007) 1222-1230.

[61] L. González-Mariscal, R. Tapia, D. Chamorro, Crosstalk of tight junction components with signaling pathways, Biochim. Biophys. Acta 1778 (2008) 729-756.

Figure legends

Fig. 1. Effects of LPA and S1P on PLD activity and permeability of HUV-EC. Panel A, [^{3}H] labelled HUV-EC were incubated with 10 μM LPA or 1 μM S1P for the indicated period of time, in the presence or absence of 1% 1-butanol added 30 min before the end of each treatment. Lipids were then extracted as described in Materials and Methods. The radioactivity of phosphatidylbutanol was expressed as percent of total phospholipid radioactivity. Results are means ± SEM of N=3 separate experiments. *, significantly different from time 0, $P<0.05$. Panel B,_ HUV-EC monolayers were treated with 10 μM LPA for the indicated period of time. HRP was added simultaneously at the beginning of experiments. Results are expressed as fold increase compared with the value for control cells

at each time-point and are means ± SEM of *N*=6 separate experiments performed in quadruplicate. *, significantly different from control cells, P<0.05. Panel C, HUV-EC were treated with 1 μM S1P as described above. Results are means ± SEM of *N*=3 separate experiments performed in quadruplicate. *, significantly different from control cells, P<0.05; †, significantly different from 1h time point, P<0.05.

Fig. 2. Effects of increased endogenous PA level on HUV-EC permeability. HUV-EC monolayers were treated with (panel A) 200 U/ml bacterial scPLD, (panel B) 25 μM propranolol, (panel C) 50 μM di-C8 PA. HRP was added simultaneously with drugs at the beginning of experiments. Results are expressed as fold increase compared with the value for control cells at each time-point and are means ± SEM of *N*=3 (panels A and B) or *N*=4 (panel C) separate experiments performed in quadruplicate. *, significantly different from control cells, P<0.05.

Fig. 3. Effects of PLD overexpression on HUV-EC permeability. Panel A, HUV-EC in 35 mm culture dishes were infected with adenovirus coding for GFP (adeno-GFP), hPLD1 (adeno-PLD1) or hPLD2 (adeno-PLD2) using a viral particles to cell number ratio of 100, or not infected (NI). After 12 h, the viruses were washed out and cells were further incubated in fresh culture medium for 60 h. Whole cell lysates were then prepared, and 10 μg of proteins were subjected to Western blotting as described in Materials and Methods using anti-PLD1 or anti-PLD2 antibodies for immunodetection. Panel B, HUV-EC cultured on Transwell filters were infected with adenovirus coding for GFP, hPLD1 or hPLD2. 12 h post-infection, media were replaced with fresh ones and cells were further incubated for 60 h. HRP was then added to the upper compartments. Results are expressed as fold increase compared with the value for control adeno-GFP cells, and are means ± SEM of *N*=6 separate experiments performed in quadruplicate. *, significantly different from adeno-GFP cells, P<0.05.

Fig. 4. Effects of PLD downregulation on HUV-EC permeability. Panel A, HUV-EC in 35 mm culture dishes were transfected with 50 nM of control siRNA, PLD1- or PLD2-siRNA, or left untreated for 8h. Then, transfection media were replaced with fresh ones. After 48 h, cells

were lyzed and proteins (30 µg per well) were subjected to Western blot analyses with anti-PLD1 or anti-PLD2 antibodies. Membranes were stripped and reprobed with anti-tubulin antibody. Blots shown (panel A, left) are representative of 3. Graphs (panel A, right) represent videodensitometric quantification of PLD1 (top) and PLD2 (bottom) blots after normalization by α- tubulin (*N*=3); *, significantly different from the three other conditions, P<0.05. Panel B, HUV-EC cultured on Transwell filters were transfected with 50 nM of control siRNA, PLD1- or PLD2-siRNA as described above. After 48 h, HRP was added to the upper compartments. Results are expressed as fold increase compared with the value for control siRNA transfected cells and are means ± SEM of *N*=2 separate experiments performed in quadruplicate. *, significantly different from control cells, P<0.05. Panels C and D, HUV-EC cultured on Transwell filters were transfected with the different siRNA and stimulated or not with 10 µM LPA for 30 min (panel C) or 2 h (panel D) before HRP flux measurement. Results are expressed as fold increase compared with the value for unstimulated control siRNA transfected cells, and are means ± SEM of *N*=2 separate experiments performed in quadruplicate. *, significantly different from control unstimulated cells, P<0.05.

Fig. 5. Effects of increased endogenous PA level or alteration of PLD expression_on actin reorganization. Panel A, HUV-EC monolayers treated for 30 min with 10 µM LPA, 1 µM S1P, 50 µM di-C8 PA or 25 µM propranolol were fixed, permeabilized and stained for actin filaments with rhodamine-conjugated phalloidin. Labelled cells were examined by fluorescence microscopy. Panel B, fluorescence microscopy of non infected HUV-EC (NI) or HUV-EC infected with adenovirus coding for GFP (adeno GFP), hPLD1 (adeno PLD1) or hPLD2 (adeno PLD2) after actin staining. Panel D, fluorescence microscopy of cells transfected with 50 nM of control siRNA, PLD1- or PLD2-siRNA and stimulated or not by 10 µM LPA for 15 min. Panels C and E, for each condition, the percentage of stress fibre positive cells was determined in at least 10 different fields. Similar results were obtained in N=2 separate experiments. In panel C, *, significantly different from the 3 other conditions, P<0.05. In panel E, *, significantly different from values without LPA, P<0.05; †, significantly different from LPA stimulated control siRNA and PLD1-siRNA transfected cells, P<0.05.

Fig. 6. Characterization of the low-density sucrose gradient fractions prepared from control HUV-EC. Triton X-100 lysates prepared from control HUV-EC were fractionated by floatation in a discontinuous sucrose density gradient, and the fraction were analyzed for (panel A) protein concentration and 5'-nucleotidase activity, (panel B) cholesterol and (panel C) GM1 content. Sucrose gradient is shown in panels B and C. Results are means ± SEM of *N*=4 separate experiments. Panel D, 30 µl of each gradient fraction mixed with Laemmli buffer were subjected to Western blot analysis using the corresponding primary antibodies.

Fig. 7. Effects of filipin on LPA-induced stress fibre formation and endothelial permeability. Panel A, HUV-EC monolayers were pretreated with 2 µg/ml filipin for 30 min or left untreated. Medium was then removed by aspiration and cells were stimulated or not by 10 µM LPA. After 15 min of LPA treatment cells were stained with rhodamine-conjugated phalloidin as described in the legend of Fig. 5. Panel B, for each condition, the percentage of stress fibre positive cells was determined in at least 10 different fields. Similar results were obtained in 2 separate experiments. Panel C, HUV-EC cultured on Transwell filters were treated or not with 2 µg/ml filipin for 30 min. Medium was then removed by aspiration and cells were stimulated or not with 10 µM LPA for 2 h before HRP flux measurement. Results are expressed as fold increase compared with the value for control untreated cells, and are means ± SEM of *N*=5 separate experiments performed in quadruplicate. *, significantly different from control cells, $P<0.05$; †, significantly different from LPA alone, $P<0.05$.

Fig. 8. Effects of PLD overexpression on occludin expression and MAP kinase phosphorylation. HUV-EC in 35 mm culture dishes were infected with adenovirus constructs coding for GFP (adeno-GFP), hPLD1 (adeno-PLD1) or hPLD2 (adeno-PLD2) using a viral particles to cell number ratio of 100, or not infected (NI). After 12 h, the viruses were washed out and cells were further incubated in fresh culture medium for 60 h. Panel A,_whole cell lysates were then prepared, and equal amounts of proteins were subjected to Western blotting using anti-occludin antibody. Panel B, videodensitometric quantification of occludin blots after normalization by α-tubulin (*N*=4); *, significantly different from the three other

conditions, P<0.05. Panel C, immunofluorescence labelling of occludin demonstrating loss of occludin at cell periphery in PLD2 overexpressing cells. Panel D, occludin mRNA levels were determined in non-infected cells and in cells infected with the various adenovirus contructs by quantitative real-time PCR. Data are expressed as fold change compared with adeno-GFP infected cells and are means ± SEM of *N*=4 independent experiments. *, significantly different from NI and adeno-GFP, P<0.05. Panels E and F, western blots of cell lysates using anti-phospho ERK antibody for immunodetection and videodensitometric quantification of phospho-ERK blots after normalization by α-tubulin (*N*=5); *, significantly different from NI and adeno-GFP, P<0.05. Panels G and H, western blots of cell lysates using anti-phospho p38 MAP kinase antibody for immunodetection and videodensitometric quantification of phospho-p38 MAP Kinase blots after normalization by α-tubulin (*N*=3); NS. Blots shown in panels A, E and G are representative of 3 to 5 separate experiments.

Fig. 9. Raf-1 mediates PA-induced ERK-1/2 activation and hyperpermeability. Panel A, HUV-EC cultured on Transwell filters were pre-treated or not with 25 μM PD98059 or with 10 μM U0126 during 30 min and cells were stimulated or not with 10 μM LPA for 2 h before HRP flux measurement. Results are expressed as fold increase compared with the value for control cells and are means ± SEM of *N*=3 separate experiments performed in quadruplicate. *, significantly different from control cells, P<0.05; †, significantly different from cells stimulated with LPA alone. Panel B, HUV-EC cultured on Transwell filters were pre-treated or not with 100 nM GW-5074 during 30 min and cells were stimulated or not with 10 μM LPA for 2 h before HRP flux measurement. Results are expressed as fold increase compared with the value for control cells and are means ± SEM of *N*=2 separate experiments performed in quadruplicate. *, significantly different from control cells, P<0.05; †, significantly different from cells stimulated with LPA alone. Panel C, HUV-EC cultured on Transwell filters were pre-treated or not with 100 nM GW-5074 for 30 min and cells were treated with 50 μM diC8-PA for 2 h before HRP flux measurement. *, significantly different from control cells, P<0.05; †, significantly different from cells stimulated with PA alone. Panel D, HUV-EC cultured on Transwell filters were infected with adenovirus constructs coding for GFP, hPLD1 or hPLD2 in the presence or absence of 100 nM GW-5074. 12 h post-infection, media

were replaced with fresh ones and cells were further incubated for 60 h. HRP permeability was measured 2h after HRP addition to the upper compartment. Results are expressed as fold increase compared with the value for control adeno-GFP cells, and are means ± SEM of *N*=4 separate experiments performed in triplicate. *, significantly different from adeno-GFP cells, P<0.05; †, significantly different from adeno-PLD2 cells cultured without GW-5074. Panels E and F, HUV-EC were pre-treated or not with 100 nM GW-5074 for 30 min and then stimulated or not with 10 μM LPA for 30 min (panel E), or with 50 μM diC8-PA for 15 min (panel F). Cell lysates were subjected to Western blotting using anti-phospho-ERK antibody for immunodetection (top). The same membrane was stripped and reprobed with anti-tubulin antibody (bottom). Panel G and H, videodensitometric quantification of phospho-ERK blots after normalization by α- tubulin (*N*=3). *, significantly different from control cells, P<0.05; †, significantly different from cells stimulated with LPA (panel G) or diC8-PA (panel H) alone, P<0.05.

Figure 1

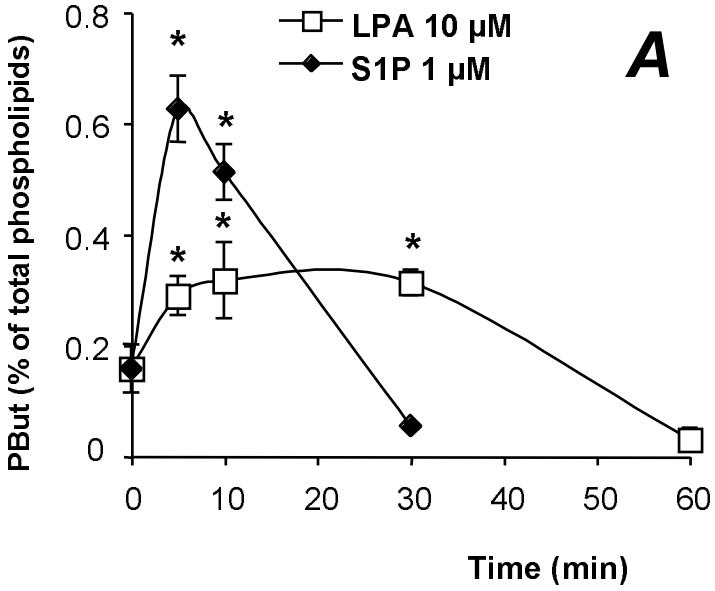
LPA 10 µM
S1P 1 µM
A
PBut (% of total phospholipids)
0.8
0.6
0.4
0.2
0
0
10
20
30
40
50
60
Time (min)

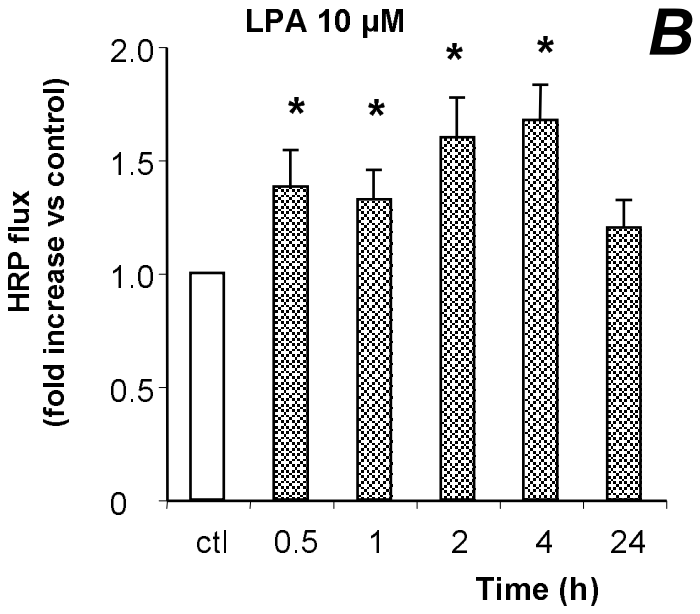
LPA 10 µM
B
HRP flux
(fold increase vs control)
2.0
1.5
1.0
0.5
0
ctl
0.5
1
2
4
24
Time (h)

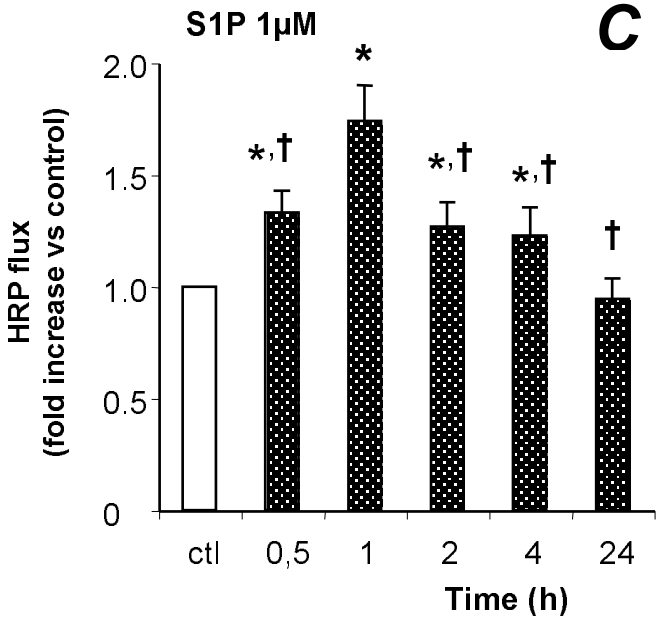
S1P 1µM
C
HRP flux
(fold increase vs control)
2.0
1.5
1.0
0.5
0
ctl
0,5
1
2
4
24
Time (h)

Figure 2

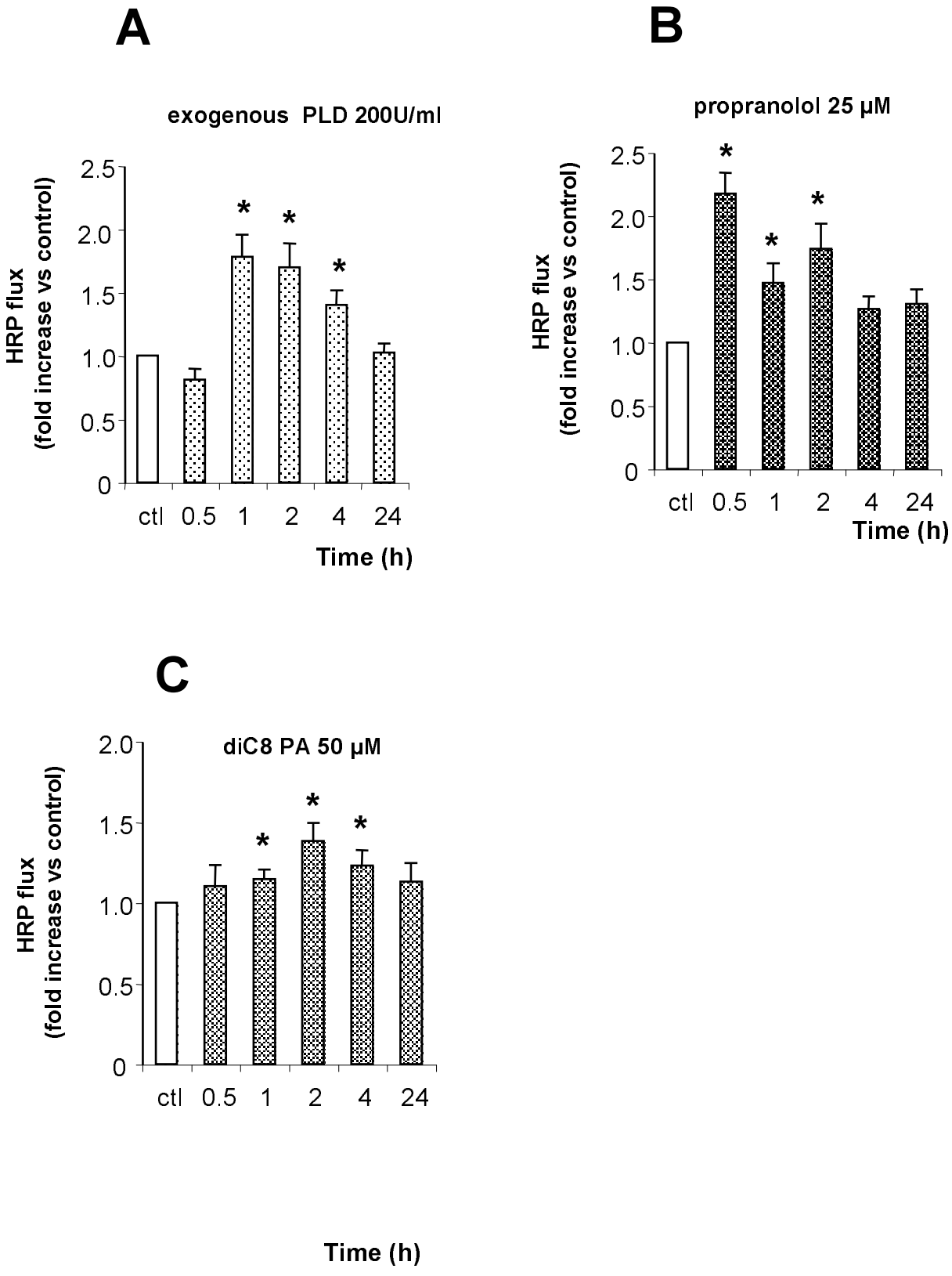
A
exogenous PLD 200U/ml
HRP flux
(fold increase vs control)
2.5
2.0
1.5
1.0
0.5
0
ctl 0.5 1 2 4 24
Time (h)
B
propranolol 25 µM
HRP flux
(fold increase vs control)
2.5
2.0
1.5
1.0
0.5
0
ctl 0.5 1 2 4 24
Time (h)
C
diC8 PA 50 µM
HRP flux
(fold increase vs control)
2.0
1.5
1.0
0.5
0
ctl 0.5 1 2 4 24
Time (h)

Figure 3

A

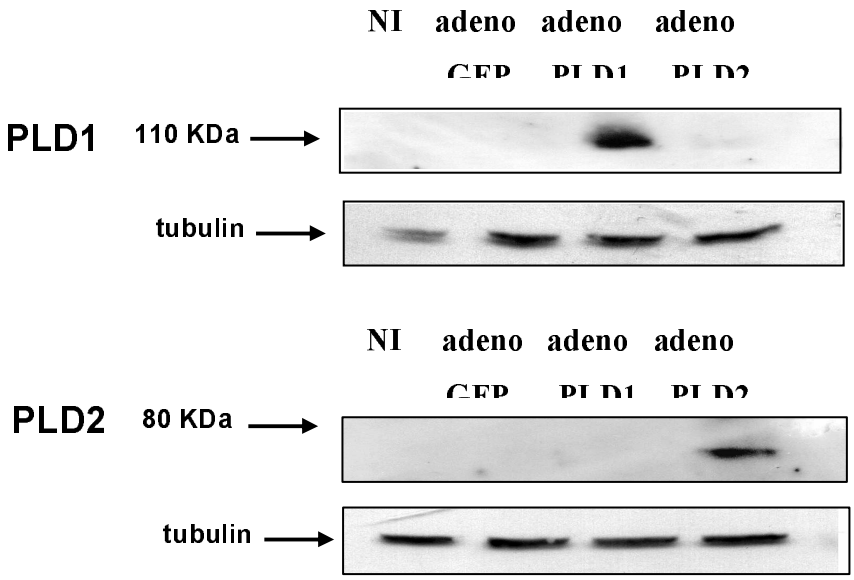
NI
adeno GFP
adeno PLD1
adeno PLD2
PLD1
110 KDa
tubulin
NI
adeno GFP
adeno PLD1
adeno PLD2
PLD2
80 KDa
tubulin

B

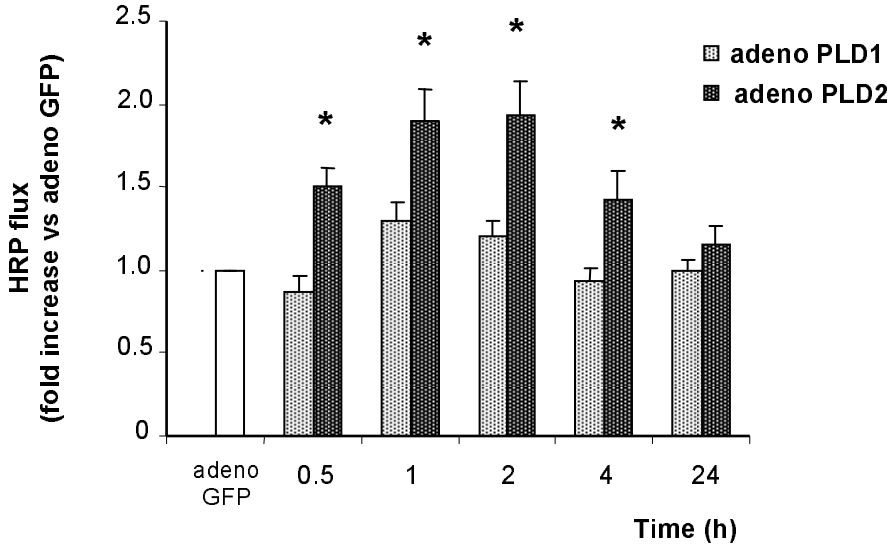
HRP flux
(fold increase vs adeno GFP)
2.5
2.0
1.5
1.0
0.5
0
adeno GFP
0.5
1
2
4
24
Time (h)
adeno PLD1
adeno PLD2
*
*
*
*

Figure 4

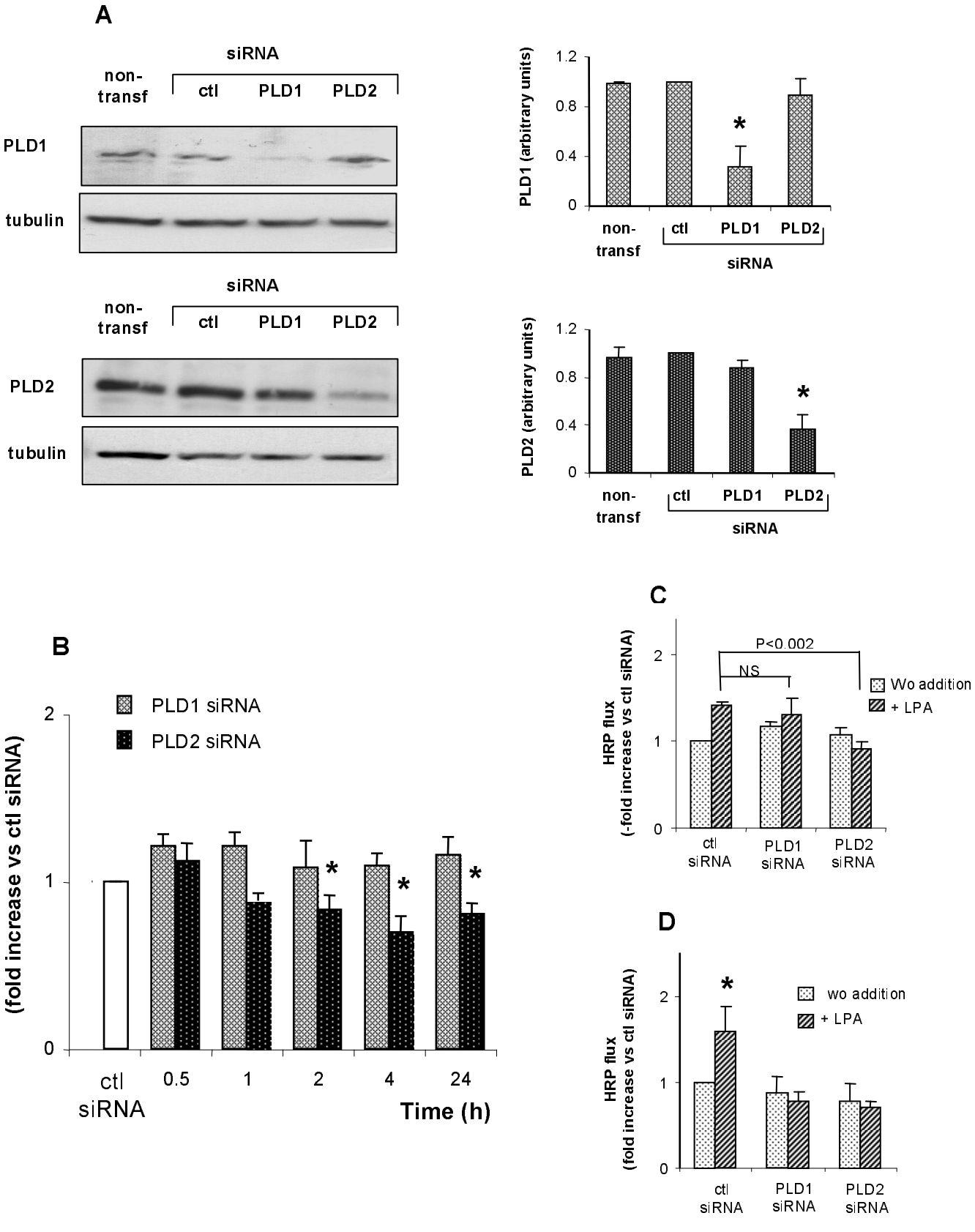
A
siRNA
non-transf
ctl
PLD1
PLD2
PLD1
tubulin
siRNA
non-transf
ctl
PLD1
PLD2
PLD2
tubulin
PLD1 (arbitrary units)
1.2
0.8
0.4
0
*
non-transf
ctl
PLD1
PLD2
siRNA
PLD2 (arbitrary units)
1.2
0.8
0.4
0
*
non-transf
ctl
PLD1
PLD2
siRNA
B
PLD1 siRNA
PLD2 siRNA
HRP flux
(fold increase vs ctl siRNA)
2
1
0
*
*
*
ctl siRNA
0.5
1
2
4
24
Time (h)
C
P<0.002
NS
Wo addition
+ LPA
HRP flux
(-fold increase vs ctl siRNA)
2
1
0
ctl siRNA
PLD1 siRNA
PLD2 siRNA
D
*
wo addition
+ LPA
HRP flux
(fold increase vs ctl siRNA)
2
1
0
ctl siRNA
PLD1 siRNA
PLD2 siRNA

Figure 5

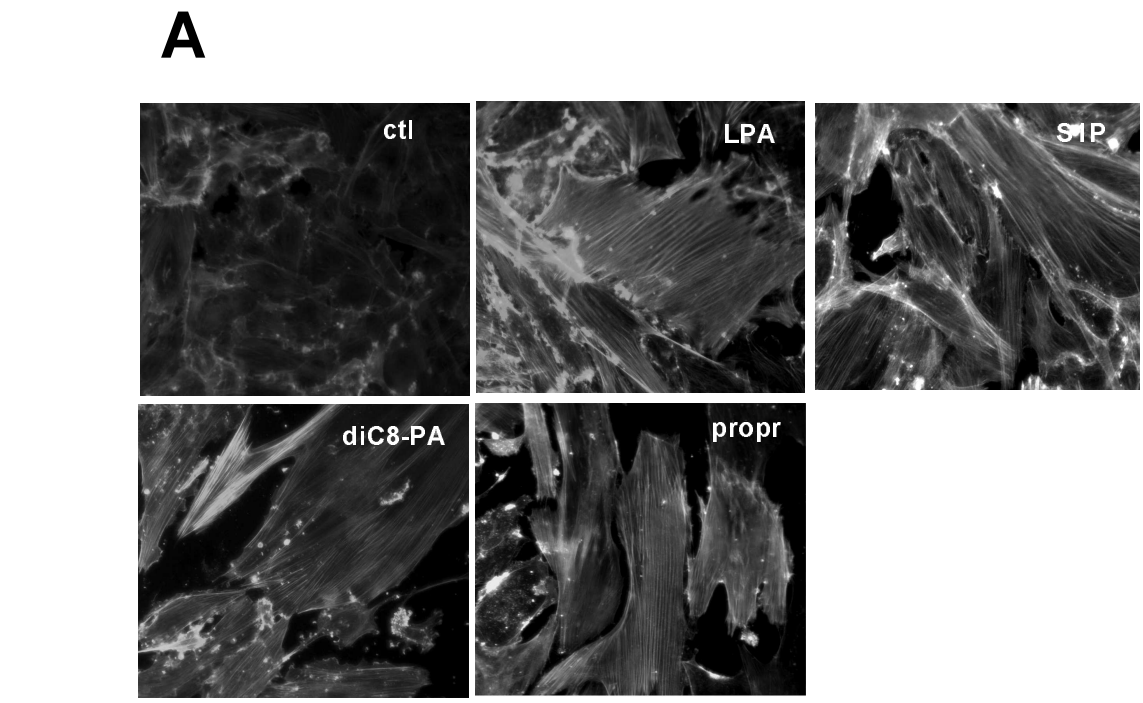
A
ctl
LPA
S1P
diC8-PA
propr
B
NI
adeno GFP
adeno PLD1
adeno PLD2
C
% of stress fibre positive cells
0
10
20
30
40
50
*
NI
adeno GFP
adeno PLD1
adeno PLD2

Figure 5 (continued)